Geotechnical and Geophysical Site Characterisation 5 – Lehane, Acosta-Martínez & Kelly (Eds)
© 2016 Australian Geomechanics Society, Sydney, Australia, ISBN 978-0-9946261-2-7

Evaluation of CPT- based ultimate lateral pile resistance in sand

H.Y. Qin
School of Computer Science, Engineering and Mathematics, Flinders University, Adelaide, Australia

W.D. Guo
School of Civil, Mining and Environmental Engineering, University of Wollongong, Wollongong, Australia

ABSTRACT: The CPT-q_c has been used quite successfully to estimate the shaft friction f_s along vertically loaded piles. This prompts the question of how to use the q_c to estimate the ultimate laterally loaded pile resistance p_u, as the correlation between q_c and p_u is not as strong as that between q_c and f_s. In this paper, modulus of subgrade reaction k and the p_u profile were deduced using closed-form solutions and measured response of eight laterally loaded rigid piles tested in-situ and in 1g model tank, respectively. A good comparison is made for each test using a constant k and linear increasing p_u. The deduced values of k and p_u are consistent with those gained previously for 57 lateral piles. Particularly, the gradient of p_u over $q_{c\_average}$ for the short piles is equal to (1.8 - 8.8)%, which is only a fraction of other suggestions. This difference necessitates further study on the correlation between q_c and p_u.

1 INTRODUCTION

Load transfer approaches using p ~ y curves are widely used to analyse the behaviour of laterally loaded piles. Several methods for the formulation of p ~ y curves for piles in sand have been put forward, in which the friction angle of the soil is generally required to estimate the ultimate soil resistance. Alternatively, the ultimate soil resistance profile may be deduced from the analysis of test results using closed-form solutions or numerical modelling. In previous study, Qin & Guo (2014a,b) investigated the nonlinear response of 57 laterally loaded rigid piles in sand. Measured response of each pile test was used to deduce input parameters of modulus of subgrade reaction and the ultimate lateral soil resistance using elastic-plastic solutions. Based on statistical analysis, an equation is presented to estimate the gradient of the ultimate lateral soil resistance with a linear variation with depth from the effective unit weight, square of the passive earth pressure coefficient and diameter of the pile.

In this paper, elasto-plastic solutions were used to analyse the response of laterally loaded rigid piles in sand obtained from new field tests, in which the cone penetration test (CPT) cone resistance q_c were measured. Results from these tests allow the ultimate soil resistance p_u profiles to be back calculated and then linked with CPT q_c values. Comparisons were also made between the back calculated p_u with those computed using the expression directly based on CPT q_c values.

2 ELASTO-PLASTIC SOLUTIONS FOR LATERALLY LOADED RIGID PILES

A pile is defined as rigid if the pile-soil relative stiffness, E_P/G_s exceeds a critical ratio, $(E_P/G_s)_c$, where $(E_P/G_s)_c = 0.052(l/r_0)^4$ and E_P is Young's modulus of an equivalent solid cylindrical pile of diameter d, G_s is the soil shear modulus, l is the pile embedded length, and r_0 is the outer radius of the pile. The elasto-plastic solutions were developed for laterally loaded rigid piles using a load transfer model (Guo 2008). As shown in Figure 1(a), the pile head is free with no constraints. The pile soil interaction is characterized by a series of springs distributed along the shaft. The spring has an elastic-plastic p ~ y (u) curve at each depth, where p is the soil lateral resistance per unit length, u is the pile deflection. The lateral resistance, p is proportional to the local pile displacement, u at that depth and the modulus of subgrade reaction, kd, i.e. p = kdu, where k is the gradient of the p ~ u curve and d is pile outer diameter. The gradient k may be written as k_0z^m, with m = 0 and 1 being referred to as constant k and Gibson k hereafter. Where the soil resistance reaches the limiting p_u, relative slip takes place along the pile-soil interface and extends to a depth z_0, which is called pre-tip yield state. With increasing load the pile-soil relative slip may also initiate from the pile tip (z = l) and expand upwards to another depth z_1 (see Figure 1(c)). The two plastic zones tend to merge at which the pile reaches the ultimate state, i.e. yield at rotation point (z_0=z_1=z_r). It is assumed that the p_u varies linearly with depth z and is described by p_u=$A_r$dz, where A_rd is the gradient of the p_u profile. The solutions allow the nonlinear responses (e.g. load, displacement, rotation and maximum bending moment) to be readily estimated, using the two parameters k and A_r. Conversely, the two parameters can be deduced from the measured pile test results. The solutions have been implemented into a spreadsheet program to facilitate calculation.

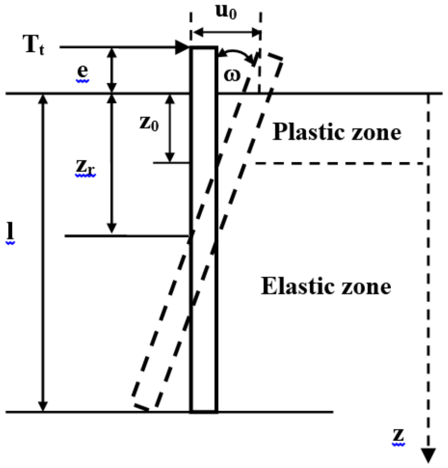

(a)

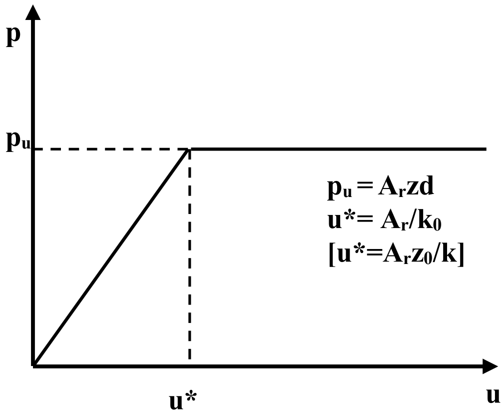

(b)

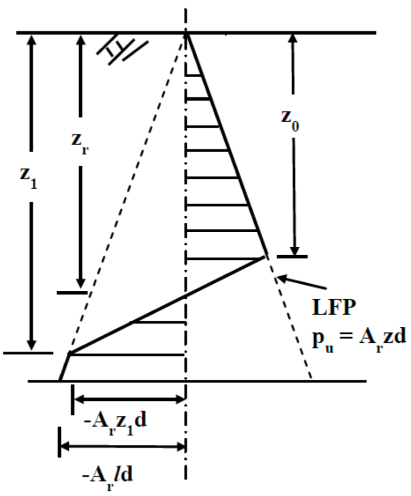

(c)

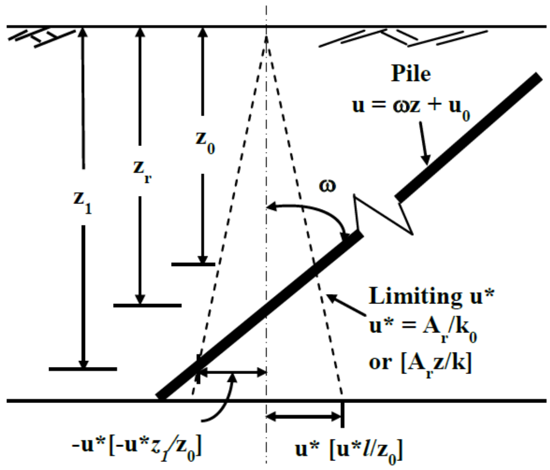

(d)

T_t = lateral load; e = eccentricity; z = depth from ground line; u_0= pile displacement at ground surface; ω = angle of rotation (in radian); u* = local threshold u above which pile soil relative slip is initiated

Figure 1. Schematic analysis for a rigid pile (after Guo (2008)) (a) pile-soil system, (b) load transfer model, (c) p_u (LFP) profiles, (d) pile displacement characteristic

3 ANALYSIS OF MEASURED PILE RESPONSES

Using the spreadsheet program, responses of eight piles in sand with the CPT q_c profiles measured at the test sites were investigated, following the same approach in Qin & Guo (2014a, b). The q_c values vary approximately linearly with depth in these tests. The properties of the piles and soils are tabulated in Table 1. Each case study is presented below.

Table 1. Summary of pile and soil properties

Test	l (m)	d (m)	e (m)	γ_s' (kN/m^3)	ϕ_s' (°)	Reference
T1	1.2	0.4	2	14.5	35.4	Lee et al. (2010)
T2	2.4	0.4	2	14.5	35.4	
T3	2.4	0.4	0.15	14.5	35.4	
1	1.2	0.4	2	18	30	Choi et al. (2013)
2	2.4	0.4	2	18	30	
4	2.4	0.4	0.15	18	30	
PS2	2.2	0.34	0.4	20	37	Li et al. (2014)
1	0.915	0.165	0.99	9.3	35.5	Zhu et al. (2015)

3.1 *Bored pile tests in weathered clayey sand*

Lee et al. (2010) reported three field tests conducted on bored piles in weathered clayey sand at Iksan, South Korea. The piles (T1, T2 and T3) have a diameter of 0.4 m with embedded depth of 1.2 m, 2.4 m and 2.4 m, respectively. The lateral load was applied at 2 m for T1 and T2, and 0.15 m for T3 above the ground level. The dry unit weight of the clayey sand is 14.5 kN/m^3 with a relative density of about 30~35 %. The peak friction angle of the soil was determined as 35.4° from triaxial tests. The measured CPT cone resistance q_c profile down the pile depth can be approximated by $q_c = 4.2 + 0.2z$, where q_c is in MPa, z in m. The measured lateral load T_t ~ pile displacement at the ground level u_0 are plotted in Figure 2(a). Back calculations were made for the three tests and the calculated pile responses (T_t ~ u_0) by best matching the measured curves are also plotted in Figure 2(a). The deduced parameters A_r, k and k_0 are presented in Table 2. The calculated ultimate loading capacities T_u are 22.3, 52.4, and 220.0 kN for tests T1, T2 and T3, respectively. They compare well with the ultimate capacities of 22, 50 and 210 kN determined from the load ~ displacement curve using the criterion suggested by Meyerhof, which defines the T_u as the load from which the displacement increases approximately linearly with load.

piles have the same diameter of 0.4 m and were installed to an embedded length of 1.2 m (Test 1), and 2.4 m (Test 2 and 4). The unit weight of the silty sand is 18 kN/m^3 corresponding to a relative density of 30~35 %. The internal friction angle and cohesion of the soil was evaluated as 30° and 20 kPa, respectively, from triaxial tests. The measured CPT cone resistance q_c profile along the embedded pile length can be estimated by $q_c = 8 + 0.335z$, where q_c is in MPa, z in m. Load was applied at an eccentricity of 2 m for Tests 1 and 2, 0.15 m for Test 4. The measured lateral load T_t ~ pile displacement at the ground level u_0 are plotted in Figure 3(a). The A_r, k and k_0 were calculated by matching the predicted and measured T_t ~ u_0 relationship. They are summarised in Table 2. Interestingly, the range of the deduced A_r, k, k_0 and T_u are similar for the same pile dimensions, ratio of loading eccentricity to pile embedded length, and similar soil properties for the tests conducted in Iksan by Lee et al. (2010) & Choi et al. (2013).

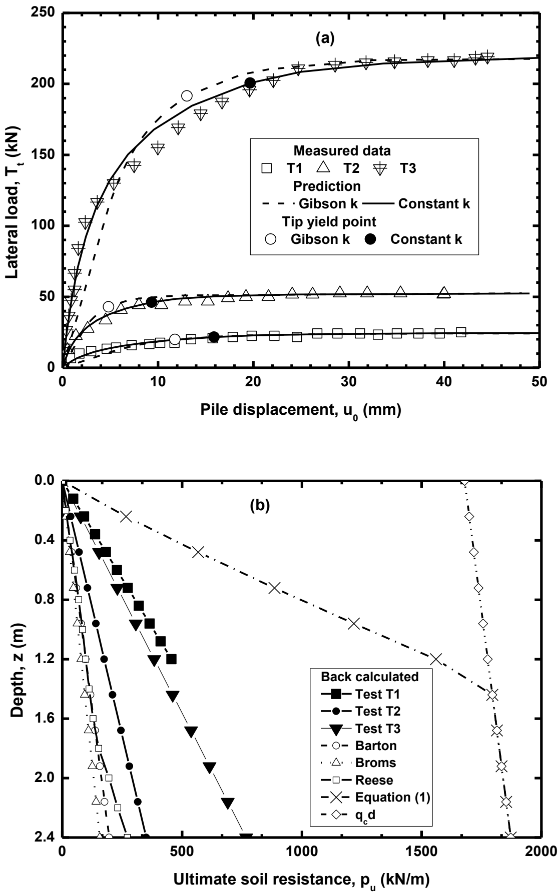

Figure 2. Predicted and measured responses of piles (Lee et al. 2010)

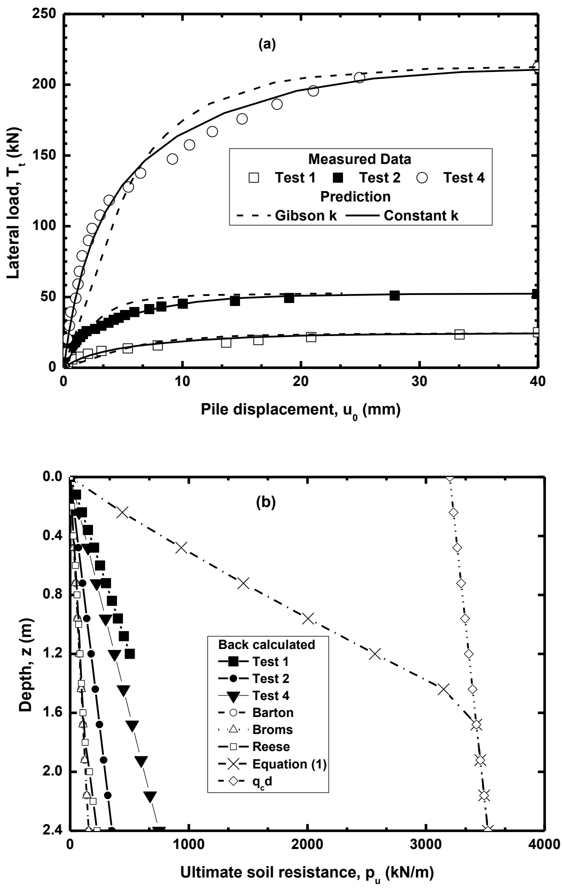

Figure 3. Predicted and measured responses of piles (Choi et al. 2013)

3.2 *Bored pile tests in weathered silty sand*

Choi et al. (2013) reported full scale field model tests of laterally loaded bored piles in weathered silty sand at Iksan city, South Korea. The model

3.3 *Driven pile tests in dense siliceous sand*

Li et al. (2014) presented a series of field lateral load tests performed on open-ended steel pipe piles driven in dense siliceous sand. The tests were conducted at the University College Dublin geotechnical test site in Blessington, Ireland. The in situ relative density was close to 100% and the unit weight of the soil was 20 kN/m^3. A constant volume friction angle of 37° was determined from triaxial compression tests and the peak friction angle decrease from 54° at 1 m depth to 42° at about 5 m depth. The averaged cone resistance q_c obtained from multiple CPTs increases approximately linearly with depth and can be described by $q_c = 10 + 5z$ between ground level and 2 m depth, where q_c is in MPa, z in m. Among these tests, the pile PS2 was driven to an embedded depth of 2.2 m and the load eccentricity was 0.4 m. The measured $T_t \sim u_0$ and the moment at ground level M0 ~ pile rotation angle ω curves are plotted in Figure 4 (a) and (b). With A_r = 850 kN/m^3, k_0 = 100 MN/m^4, k = 108 MN/m^3, the predicted $T_t \sim u_0$ and $M_0 \sim \omega$ relationships compare well with the measured data. Nevertheless, the maximum bending moment was overestimated by about 35% at T_t =101 and 110 kN in Figure 4(c). The comparison also shows that the solution with a Gibson k offers a better estimation against measured $T_t \sim u_0$ curve (within u_0 of 5% of the pile diameter) than that based on constant k for the same A_r. This reveals that the assumption of Gibson k may suit very dense sands with very high relative density, for instance, close to 100% in this test.

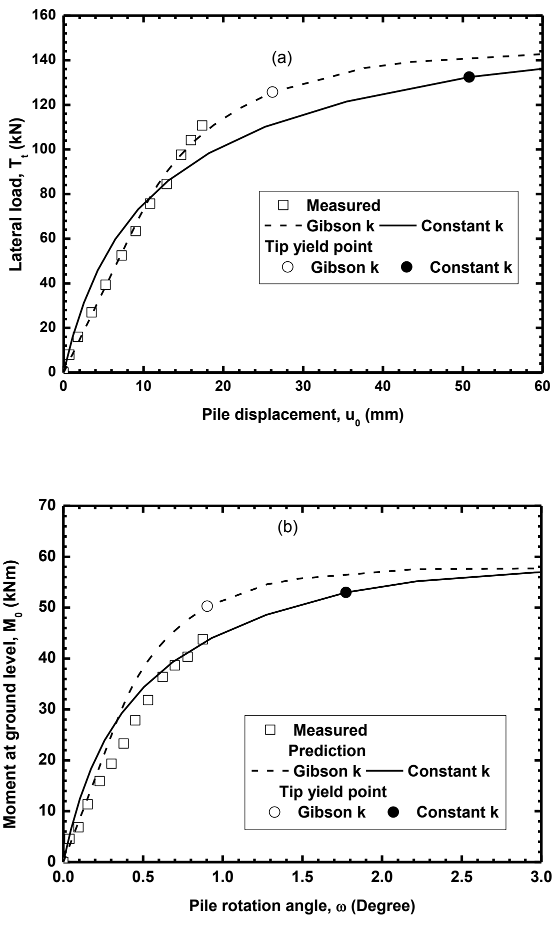

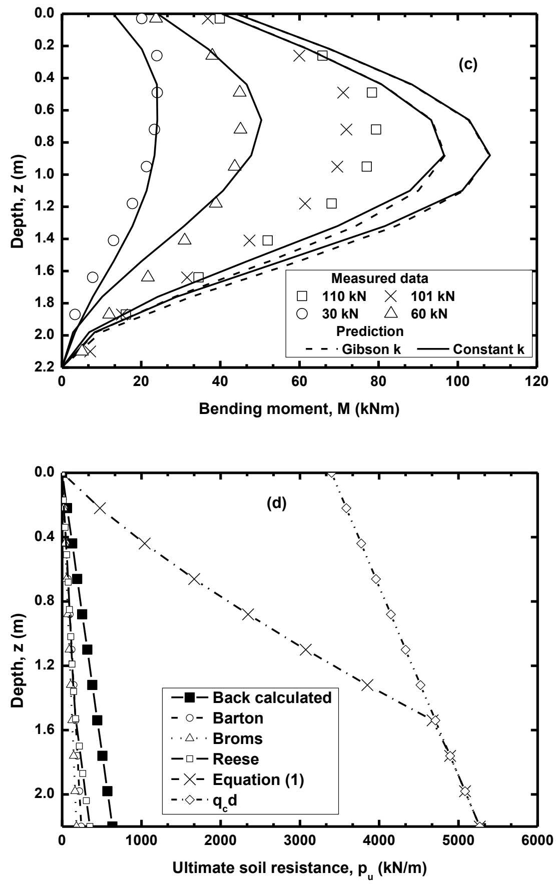

Figure 4. Predicted and measured responses of piles (Li et al. 2014)

3.4 *Laboratory model pile tests in sandy silt*

Zhu et al. (2015) reported a series of 1-g model tests on an instrumented rigid pile subjected to lateral loads. The response of their Test 1 was analysed in this study. The model steel pipe pile has an embedded length of 0.915 m and diameter of 0.165 m. The load eccentricity is 0.99 m (i.e. e = 5d). The tests were carried out in sandy silt under submerged condition. The soil has a saturated unit weight of 19.1 kN/m^3, relative density of 88%, effective peak and residual frictional angle of 41.5° and 35.5°, respectively. The measured CPT cone resistance q_c profile along the embedded pile length can be estimated by $q_c = 3.0z$, where q_c is in MPa, z in m. The measured $T_t \sim u_0$ curve is plotted in Figure 5 (a). The measured pile displacement under load T_t of 736, 992, 1452, 1522 N are plotted in Figure 5(b). The measured soil pressure on the pile using pressure transducers at T_t = 1522 kN is plotted in Figure 5(c). The back-calculated pile responses by best matching all the measured curves are also plotted in Figure 5 (a)-(c). This was achieved by taking A_r = 220 kN/m^3, k_0 = 26.5 MN/m^4, k = 16.5 MN/m^3. It is worth noting that the measured load T_t = 1452 N is close to the calculated T_t = 1435 N (constant k), but slightly (9%)

greater than T_t= 1330 N (Gibson k) at the tip yield state. This means that the pile may be in post-tip yield state at T_t = 1522 kN. The on-pile force profiles at T_t = 1522 N in Figure 5 (c) was obtained by using z_0/l = 0.59, z_r/l = 0.72, z_1/l = 0.93 for constant k and 0.56, 0.73 and 0.91, respectively, for Gibson k. Using the elastic-plastic model, the ultimate soil resistance increases linearly, following closely with measured soil pressure in Figure 5 (c), from zero at groundline to the maximum value at the slip depth z_0. Afterwards, the resistance decreases with depth and becomes zero at the pile rotation depth z_r. The soil pressure distribution proposed by Prasad & Chari (1999) was also included for comparison. The measured data fall within the zones enclosed by the individual soil pressure profile, indicating the pile was at tip yield state or post-tip yield state.

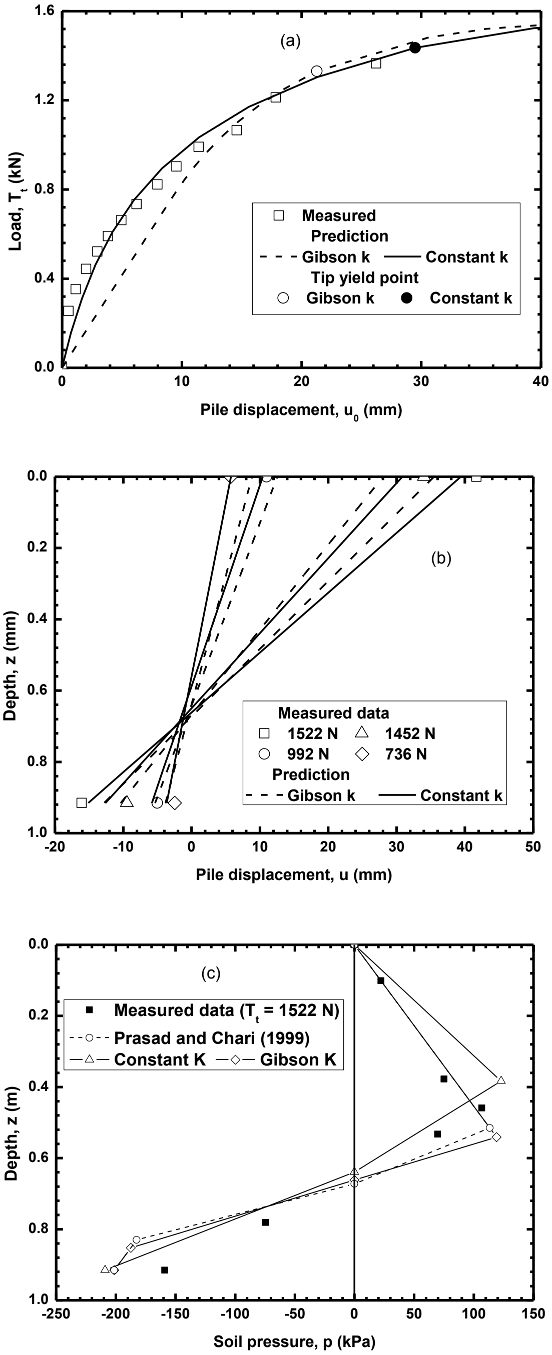

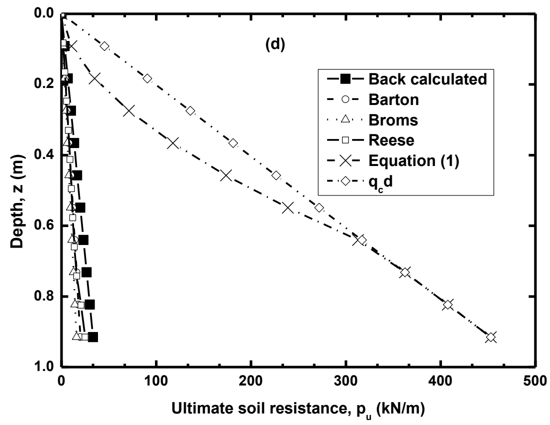

Figure 5. Predicted and measured responses of piles (Zhu et al. 2015)

Table 2. Summary of back calculated parameters

Test	A_r (kN/m^3)	N_g	k_0 (†)	k (*)	q_{c_ave} (kPa)	A_rd/q_{c_ave} (%)
T1	950	4.7	184	220	4320	8.8
T2	365	1.8	234	200	4440	3.3
T3	800	3.9	304	200	4440	7.2
1	1050	6.5	206.5	186	8201	5.1
2	368	2.3	206.5	197	8402	1.8
4	780	4.8	206.5	297	8402	3.7
PS2	850	2.6	108	100	12750	2.3
1	220	1.7	26.5	16.5	1372	2.6

† in MN/m^4, * in MN/m^3

4 ESTIMATION OF P_U PROFILE FROM CPT CONE RESISTANCE

To facilitate comparison, a non-dimensional parameter N_g is defined as $N_g = A_r/\gamma_s'K_p^2$, where γ_s' is the effective unit weight of the soil (dry unit weight above water table, and buoyant unit weight below); $K_p = \tan^2(45°+\phi_s'/2)$, is the coefficient of passive earth pressure; ϕ_s' is the effective frictional angle. The N_g was calculated for each pile test and tabulated in Table 2. Excluding the Test 1 by Choi et al. (2013), the values of N_g varies from 1.7 to 4.8, which is within the range determined previously by Qin & Guo (2014a,b) from the analysis of 57 pile test results.

The deduced p_u profiles are plotted in Figures 2(b), 3(b), 4(d), and 5(d), together with those using Broms' $p_u = 3\gamma_s'K_p dz$, (i.e. $N_g = 3/K_p$) (Broms 1964), Barton's $p_u = \gamma_s'K_p^2 dz$ (i.e. N_g = 1) (Barton 1982) and Reese's p_u profile (Reese et al. 1974). Recently, Suryasentana & Lehane (2014, 2016) proposed to estimate the p_u of a circular pile in cohesionless soils from the CPT cone resistance q_c by

$$p_u = 2.4\gamma_s' zd\left(\frac{q_c}{\gamma_s' z}\right)^{0.67}\left(\frac{z}{d}\right)^{0.75} \le q_c d \qquad (1)$$

Using the q_c distribution, the ultimate soil resistance p_u was calculated and plotted in these figures as well. The comparison shows that the p_u calculated from equation (1) significantly overestimates those back calculated for all the tests as well as those calculated from Broms, Barton and Reese methods, thus resulting in over prediction of ultimate lateral capacity. Equation (1) is associated with hardening CPT-based p ~ y curves. Guo & Zhu (2005) investigated the effect of using different shapes of p ~ y curves on the difference in predicted pile response for static and cyclic laterally loaded piles in calcareous sand. Their results show that p ~ y curves from the two models, elastic-perfectly plastic as in Figure (1b) and hardening p ~ y curves like those proposed by Suryasentana & Lehane (2014, 2016), offer similar pile-head displacement, maximum bending moment, distribution of pile displacement and bending moment. However, the p ~ y models affect remarkably the distribution of soil reaction, especially within the upper few diameters of the pile. For the eight pile tests, the embedded length is relatively short (maximum 2.4 m), the average q_c along the embedded pile depth may be used to estimate the gradient of the linear p_u profile, $A_r d$. Using the calculated $q_{c\_average}$, this leads to $A_r d = (1.8 - 8.8)\%\ q_{c\_average}$.

5 CONCLUSION

The responses of laterally loaded piles in sand were back calculated using elastic-plastic solutions against the results from field test, in which the CPT q_c were measured. Eight case studies demonstrate that, with elasto-plastic p ~ y curves, the pile responses can be well predicted. The assumption of Gibson k may be suitable for very dense sands. Comparison among the back calculated and existing p_u profiles indicates that the expression proposed by Suryasentana & Lehane (2014, 2016) may overestimate the ultimate lateral resistance. The analyses allow the gradient of the linear ultimate lateral resistance profile for sand to be calculated directly from the average cone resistance q_c along the pile embedded depth by $A_r d = (1.8 - 8.8)\%\ q_{c\_average}$. However, this equation is obtained from relative short piles with small diameter. More case studies available will be helpful to refine this equation.

6 ACKNOWLEDGEMENTS

The authors thank Dr Weichao Li for providing the measured data in Figure 4(c).

7 REFERENCES

Broms, B.B. 1964. Lateral resistance of piles in cohesiveless soils. *Journal of Soil Mechanics and Foundation Engineering* 90(3): 123-156.

Barton, Y.O. 1982. Laterally loaded model piles in sand : centrifuge tests and finite element analysis. *Ph.D. thesis, University of Cambridge*.

Choi, H.Y., Lee, S.R., Park, H.I., & Kim, D.H. 2013. Evaluation of lateral load capacity of bored piles in weathered granite soil. *Journal Geotechnical and Geoenvironmental Engineering* 139(9): 1477-1489.

Guo, W.D. 2008. Laterally loaded rigid piles in cohesionless soil. *Canadian Geotechnical Journal* 45(5): 676-697.

Guo, W.D. & Zhu, B.T. 2004. Static and cyclic behaviour of laterally loaded piles in calcareous sand. In S. Gourvence & M. Cassidy (ed.), *Frontiers in Offshore Geotechnics*; *Proc. ISFOG, PERTH, 19-21 SEPTEMBER 2005*. London: CRC.

Lee, J.H., Park, H.I., Kim, M.K., & Kyung, D.Y. 2010. Estimation of lateral load capacity of rigid short piles in sands using CPT results. *Journal Geotechnical and Geoenvironmental Engineering* 136(1): 48-56.

Li, W., Igoe, D., & Gavin, K. 2014. Evaluation of CPT-based p-y models for laterally loaded piles in siliceous sand. *Geotechnique Letters* 4(2): 110-117.

Prasad, Y.V.S.N. & Chari, T.R. 1999. Lateral capacity of model rigid piles in cohesionless soils. *Soils and Foundations* 39(2): 21-29.

Qin, H.Y. & Guo, W.D. 2014a. Nonelinear response of laterally loaded rigid piles in sand. *Geomechanics and Engineering* 7(6): 679-703.

Qin, H.Y. & Guo, W.D. 2014b. Limiting force profile and laterally loaded rigid piles in sand. *Applied Mechanics and Materials* 553: 452-457.

Reese, L. C., Cox, W. R., & Koop, F. D. 1974. Analysis of laterally loaded piles in sand. *Proc., 6th Annual Offshore Technology Conf.,Vol.* 2: 473–483.

Suryasentana, S.K. & Lehane, B.M. 2014. Numerical derivation of CPT-based p-y curves for piles in sand. *Geotechnique* 64(3): 186-194.

Suryasentana, S.K. & Lehane, B.M. 2016. Updated CPT-based p-y formulation for laterally loaded piles in cohesionless soil under static loading. *Geotechnique* 66(6): 445-453.

Zhu, B., Sun, Y.X., Chen, R.P., Guo, W.D., & Yang, Y.Y. 2015. Experimental and analytical models of laterally loaded rigid monopoles with hardening p-y curves. *Journal Waterway, Port, Coastal, and Ocean Engineering* 141(6): 04015007-1-04015007-11.